energies

MDPI

Article

Control Structures for Combined H_2/Electricity from Offshore Wind Turbines

José Luis Monroy-Morales [1,*], Rafael Peña-Alzola [2,*], David Campos-Gaona [2] and Olimpo Anaya-Lara [2]

[1] Graduate Program and Research in Electrical Engineering, TecNM/Instituto Tecnológico de Morelia, Av Tecnológico, No. 1500, Morelia C.P. 58120, Mexico
[2] Electronic and Electrical Engineering, University of Strathclyde, 204 George St., Glasgow G1 1XW, UK; d.campos-gaona@strath.ac.uk (D.C.-G.); olimpo.anaya-lara@strath.ac.uk (O.A.-L.)
* Correspondence: jose.mm@morelia.tecnm.mx (J.L.M.-M.); rafael.pena-alzola@strath.ac.uk (R.P.-A.); Tel.:+52-4434641595 (J.L.M.-M.)

Abstract: Wind energy proves to be a highly favourable choice for electricity generation due to its clean and renewable nature, and is playing a significant role in reducing global greenhouse gas emissions. Offshore wind turbine systems have gained widespread popularity as they can capitalise on elevated and consistent wind speeds surpassing those found in onshore locations, resulting in increased energy efficiency. Furthermore, offshore wind power possesses the potential to emerge as a significant electricity source for the production of green hydrogen. As water electrolysis technology for hydrogen production continues to advance, utilizing offshore wind power for hydrogen generation is becoming more economically viable and practical. Offshore wind power with higher wind speeds in combination with efficient control structures presents an attractive option for electricity generation and hydrogen co-production. This paper aims to present and evaluate four different production structures for combined H_2/energy generation from offshore wind turbines. Previous research studies in this area often overlook control structures and lack information on power converter operations. In contrast, this article studies control structures that enable proper functionality and ensure adequate interoperability, enhancing the reliability of renewable energy integration. Each structure, including both wind turbines and electrolyser, is described in detail, along with the corresponding controllers. Simulation results are presented for each structure and controller to demonstrate their effective operation.

Keywords: offshore; onshore; green hydrogen; wind turbines; DFIG

Citation: Monroy-Morales, J. L.; Peña-Alzola, R.; Campos-Gaona, D.; Anaya-Lara, O. Control Structures for Combined H_2/Electricity from Offshore Wind Turbines. *Energies* **2024**, *17*, 5353. https://doi.org/10.3390/en17215353

Academic Editor: Davide Astolfi

Received: 1 October 2024
Revised: 22 October 2024
Accepted: 26 October 2024
Published: 28 October 2024

1. Introduction

Wind power has increased significantly as a replacement for the systems using fossil fuels, helping to achieve a decarbonised world [1–3]. The implementation of offshore wind farms has increased, as they produce more power than onshore wind farms due to offshore wind speeds being higher and more consistent [4]. In addition, offshore wind farms present several advantages: (a) wind energy is an infinite and environmentally friendly source of power; (b) offshore locations offer more abundant wind resources compared to onshore sites, with potential yields up to double that of a medium-sized onshore wind farm; (c) offshore wind farms have minimal visual and acoustic impact, allowing for the utilization of larger areas; (d) offshore wind farms typically have installed capacities in the range of several hundred megawatts; and (e) offshore wind turbines are capable of achieving significantly larger unit capacities and sizes compared to onshore wind turbines [5–7]. Wind turbines are dependent on intermittent wind speeds and subject to weather conditions, representing a challenge with respect to control of energy demand [8]. These generators may produce electricity during periods of low demand or fall short during periods of high demand. Hydrogen can assist in addressing of the period of low demand by utilising excess electricity for hydrogen production [9].

As of 2020, a significant portion of hydrogen production (approximately 96%) is reliant on natural gas, leading to substantial CO_2 emissions [10]. Therefore, in order to mitigate climate change resulting from the worldwide rise in CO_2 emissions, it is imperative to develop methods for producing carbon-neutral and sustainable fuels. A viable solution is the production of green hydrogen, which involves utilising a renewable energy source to generate electricity for the process of water electrolysis.

The production of green hydrogen through electrolysis using renewable sources involves the decomposition of water molecules (H_2O) into oxygen (O_2) and hydrogen (H_2) [11–15]. Green hydrogen generation offers several advantages:

- It is entirely sustainable, as it does not emit any polluting gases during combustion or production, making it an environmentally friendly option.
- Hydrogen is easily stored, allowing for its utilization at later times and for various purposes beyond immediate production.
- Green hydrogen can be converted into electricity or synthetic gas, enabling its application in diverse commercial, industrial, and mobility sectors, further enhancing its versatility and usefulness.

Hence, green hydrogen stands out as a highly promising carrier for renewable energy [16,17].

In this paper, four control structures for offshore wind turbine hydrogen production are presented. The first structure transports electricity generated by the offshore wind turbine to onshore facilities through an AC line, where part of this electricity is transformed into hydrogen onshore. The second structure transports electricity through an AC line and hydrogen through a pipeline, with part of the produced electricity being transformed into hydrogen offshore. In the third structure, all of the electricity generated by the wind turbine is converted into hydrogen and transported through a pipeline. This hydrogen can be stored onshore or transformed back into electricity. The last structure uses an AC–DC converter to transport direct current from offshore to onshore; once onshore, the DC is transformed into AC and hydrogen. Simulation results for each structure are presented to corroborate the model's proper operation.

2. Main Components for H_2/Electricity Production

This section describes the components employed in each of the hydrogen generation structures discussed in this article, including commonly utilized generators in wind turbines, rectifiers, and buck converters.

2.1. Wind Turbine

Without loss of generality, the type of wind turbine selected for the simulations was based on the Doubly-Fed Induction Generator (DFIG) exemplified in Figure 1. Selecting Type 4 wind turbines based on full-rated converters using multiple synchronous machines would not modify the outcomes of this manuscript. DFIGs prove to be a reliable option, facilitating variable-speed operation within a limited range that enables efficient energy capture across various wind speeds. Moreover, DFIGs contribute to enhanced grid stability and control, offering the capability to provide both active and reactive power control. The control of DFIG-based wind turbines is well known, and details can be found in [18–22]. In this article, the DFIG is utilized in structures 1 and 2, while structures 3 and 4 utilise a wind turbine based on synchronous machines using a full rated inverter connected to a DC link.

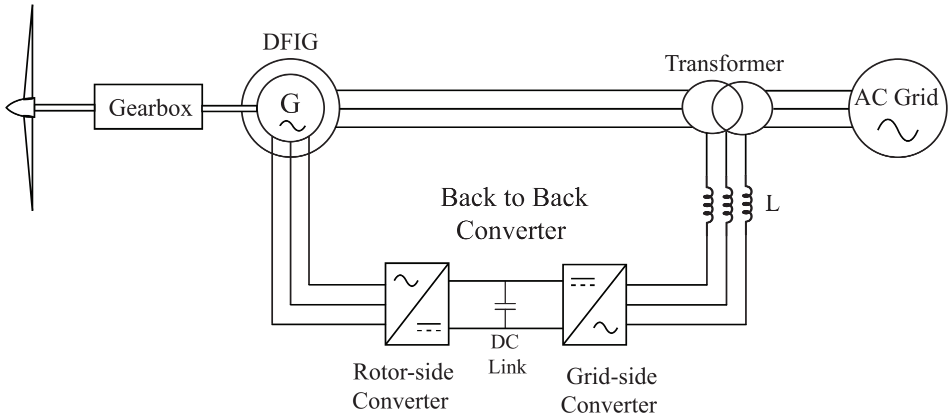

Figure 1. Doubly-Fed Induction Generator (DFIG).

2.2. *Active Rectifier for the Electroliser*

An active rectifier based on a full-bridge converter is used to convert alternating current (*ac*) into direct current (*dc*) for use by the electrolyser. An active rectifier such as the one shown in Figure 2 allows for obtaining sinusoidal currents with unity power factor. Its control is also well known, with details available in [23–27].

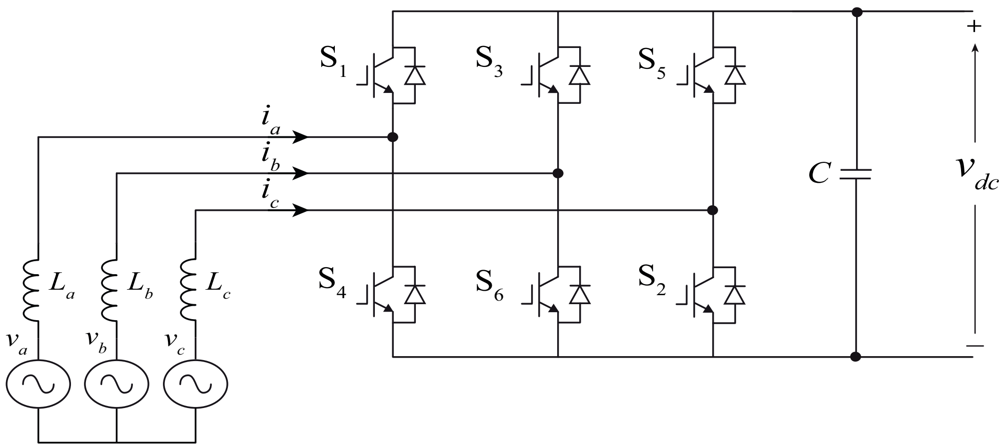

Figure 2. Three-phase active rectifier based on IGBTs.

2.3. *Synchronous Buck Converter and Electrolyser*

A synchronous buck converter is employed to achieve accurate control of the DC current provided to the electrolyser, allowing for regulation of the H_2 production flow rate [28,29]. The synchronous buck converter shown in Figure 3 replaces the conventional lower diode with a power MOSFET, which features a lower on-voltage drop compared to the forward drop of the rectifier, resulting in improved efficiency [30,31]. A synchronous buck converter uses nested controllers for current and voltage. It can use peak current mode or average control; details can be found in [32,33]. The most economically appropriate type for use in energy storage systems are alkaline water electrolysers. The decomposition of water into hydrogen and oxygen is achieved by passing a DC electricity current between two electrodes separated by an aqueous potassium hydroxide (KOH) electrolyte with good ionic conductivity [34]. This type of electrolyser is used in the proposed system because it is a mature and proven technology with high durability and relatively low cost. However, the utilisation of other electrolyser technologies such as Proton Exchange Membrane (PEM) would not change the outcomes of this study.

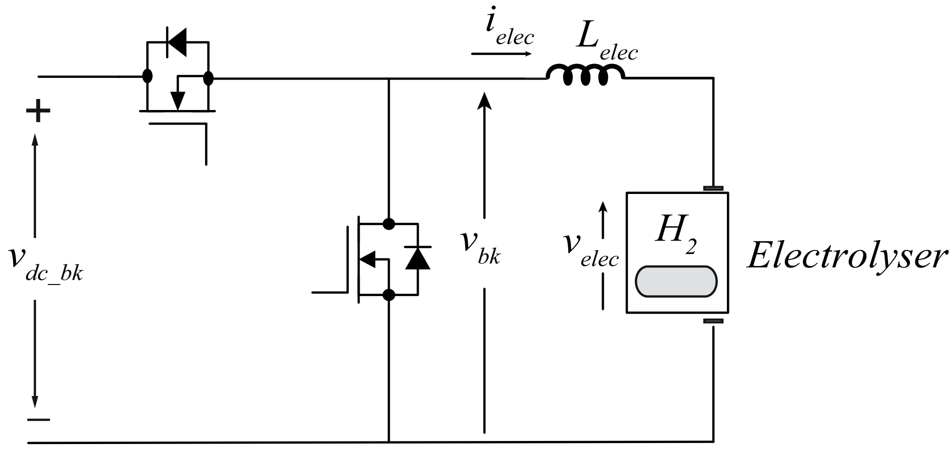

Figure 3. Synchronous Buck converter used as the electrolyser.

3. Models of the Structures for Production of H_2/Electricity

This section describes the various configurations selected for the joint production of electricity and H_2 using offshore wind turbines.

3.1. Structure 1

In the first structure, the offshore wind turbine produces only electricity, which is transmitted to the coast through an AC line. Upon arrival onshore, a significant portion of this electrical power is converted into hydrogen using an electrolyser, while a smaller fraction is retained in its original electrical state to feed local loads. The produced hydrogen is stored for subsequent utilisation. Figure 4 shows the components forming the structure.

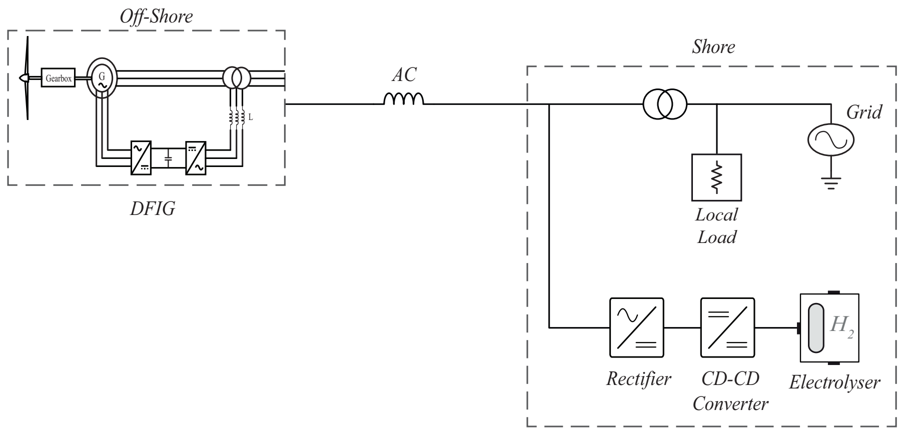

Figure 4. Structure 1: The offshore wind turbine produces only electricity, which is transmitted to the coast through an AC line.

The fundamental purpose of implementing this structure is to maximize the production of hydrogen from the marine environment using conventional AC. This hydrogen is classified as “green hydrogen” due to its originating from environmentally friendly and pollution-free renewable energy source.

As shown in Figure 4, the wind turbine is connected to a DFIG, which is responsible for producing the *AC* electrical energy that is transmitted to the coastline. This configuration requires converting *AC* into *DC* onshore through a three-phase bridge rectifier. Subsequent to the rectification process, a *DC–DC* converter is employed to efficiently regulate the *DC* current, and thereby the production of H_2 in the electrolyser.

3.2. Structure 2

The second structure still uses AC for the transmission of electrical energy; what distinguishes this structure is its added ability to facilitate the transportation of hydrogen generated from offshore locations through a pipeline, as shown in Figure 5.

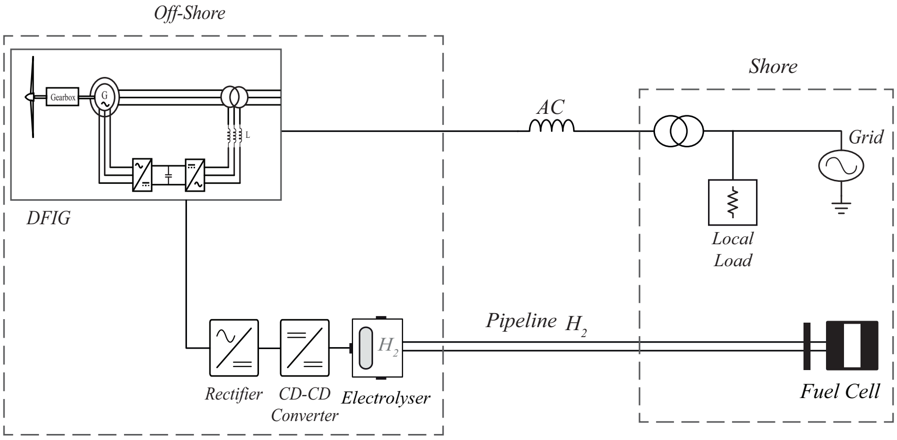

Figure 5. Structure 2: The offshore wind turbine produces electricity and H_2, which are transported to the coast through an AC line and pipeline, respectively.

This approach combines the versatility of electricity transmission with the convenience of hydrogen transport via pipeline. The compression system used for hydrogen transportation, which includes hydraulic and mechanical elements such as centrifugal pumps, pipelines, and tank stations, is modelled using MATLAB's Simscape library.

If a Type-4 wind turbine is used for the structure instead, the DC–DC converter of the electrolyser can use the DC-link present in the full-rated converter. The active rectifier of the electrolyser is not needed, reducing the cost, encumbrances, and losses.

3.3. Structure 3

In Structure 3, as shown in Figure 6, all of the power produced by the offshore wind turbine is converted and transported as hydrogen. Therefore, this configuration employs a wind turbine with a full-rated converter driving a Permanent Magnet Synchronous Generator (PMSG) for electricity generation. The DC–DC converter of the electrolyser is connected to the DC link, and regulates H_2 production.

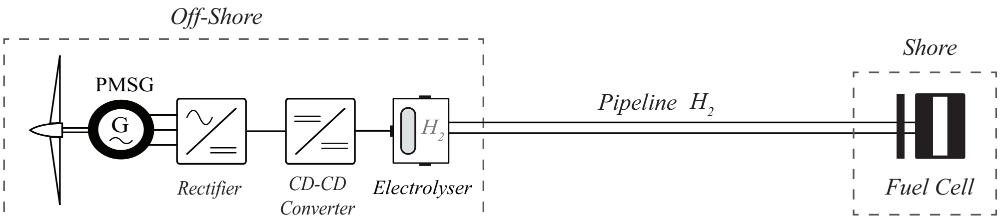

Figure 6. Structure 3: All of the power produced by the offshore wind turbine is converted and transported as H_2.

Transporting hydrogen instead of electricity is particularly advantageous for long distances, as it results in lower losses and fewer technical challenges compared to AC or DC transmission. However, all the H_2 infrastructure is offshore, which incurs additional costs and maintenance difficulties. The overall system also requires a desalination plant to obtain the purified H_2O needed by the electrolyser.

3.4. Structure 4

In Structure 4, the electrical power generated by the wind turbine is conveyed using direct current, as shown in Figure 7 in a simplified manner. Similar to Structure 3, a wind turbine with a synchronous machine controlled through a full-rated converter is employed. Transporting *DC* from offshore for hydrogen production eliminates the need for *AC–DC* conversion, thereby reducing energy losses associated with multiple conversion steps. There is no need for a rectifier for the electrolyser, which can be connected directly to the DC line for H_2 production.

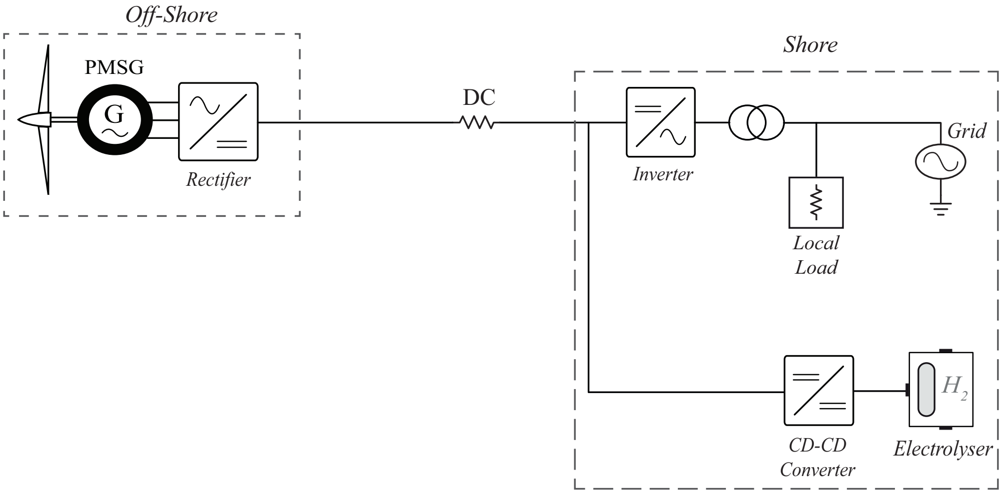

Figure 7. Structure 4: The electrical power generated by the wind turbine is conveyed using DC.

4. Control for Offshore Wind Turbines

This section outlines the control mechanisms utilized in the hydrogen generation structures discussed in the preceding section.

In the cases of Structure 1, 2, and 4 (the first case study), it is assumed that 80% of the power generated by the wind turbine undergoes conversion into hydrogen at the coastal site and that the remaining 20% is retained as electricity to meet the demand of electrical loads, as shown in Figure 8.

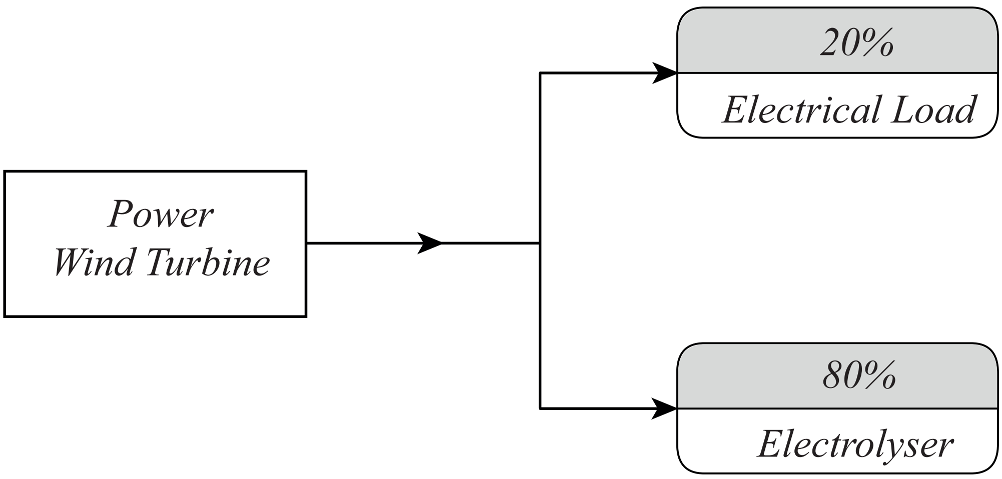

Figure 8. Power distribution.

This initiative aims to maximize the utilization of offshore wind power by converting the majority of the power produced by the wind turbine into green hydrogen.

The control diagram for the rectifier shown in Figure 2 is illustrated in Figure 9. The controller uses a voltage-oriented control (VOC) synchronised to the grid by a phase-locked loop (PLL), with inner d-q current loops and an outer DC-voltage loop. Active rectifiers connected through long AC lines can also be controlled as grid-forming converters to enhance stability. Hence, the active rectifier maintains the DC-voltage supply constant at the input of the DC–DC converter of the electrolyser.

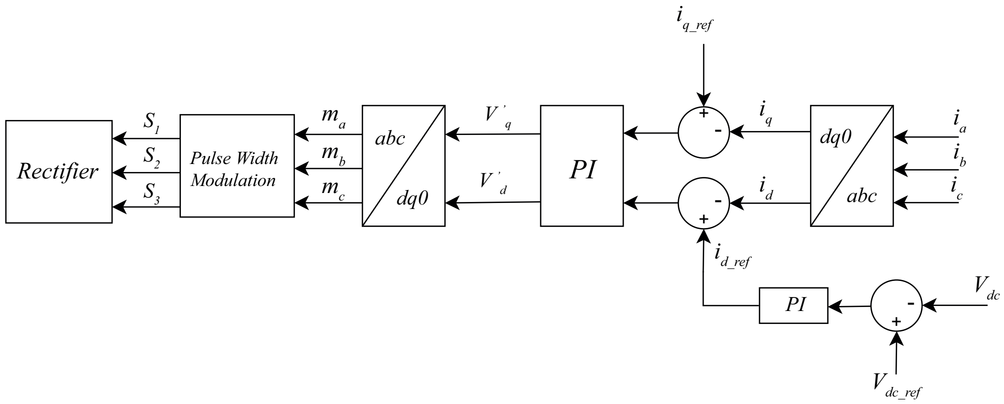

Figure 9. Voltage-oriented control of the three-phase active rectifier.

There are two approaches for ensuring that the electrical load requirements are fulfilled. In the first approach, the controller considers 80% of the wind power production estimated from onshore measurements for hydrogen production, denoted as (P_{WT}) in Figure 10. The controller regulates the output power at the DC–DC converter of the electrolyser. A slow integral controller produces the current reference for the DC–DC converter of the electrolyser; P_{WT} is divided by the electrolyser voltage, which is used as a feed-forward component to enhance dynamics in the synchronous buck-boost converter. The second approach consists of providing a fixed amount of power for the local load, with the excess energy being used for hydrogen production. The control mechanisms to prioritize hydrogen production and prioritize electrical load are shown in Figures 10 and 11, respectively.

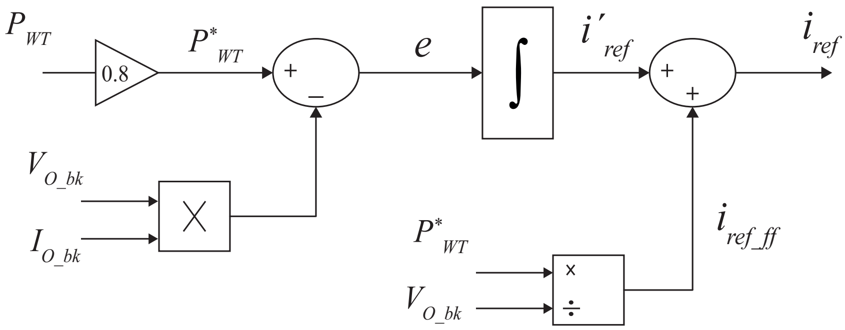

Figure 10. Control mechanism to prioritize hydrogen production.

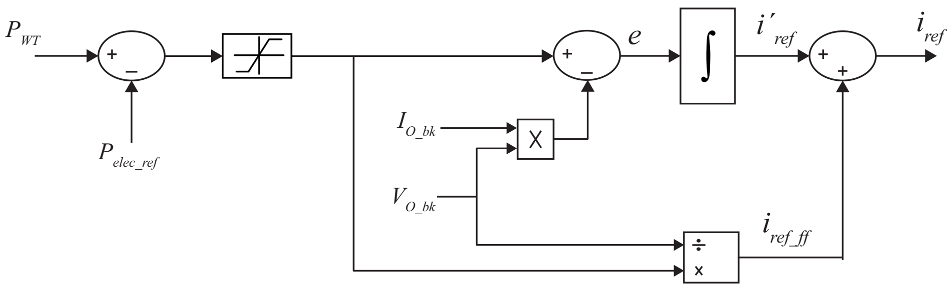

Figure 11. Control mechanism to prioritize electrical load.

5. Simulations Results

The four structures described in Section 3 were verified through software simulation using MATLAB/Simulink to validate the proposed features and assess their proper functioning.

For Structures 1, 2, and 4, the simulations involved varying the wind speed and considering two distinct case studies. In the first case study, the primary focus was on converting the electrical energy produced by the wind turbine into hydrogen, with the remaining energy supplied to the grid. In the second case study, the first priority was to supply electrical loads, with any surplus wind turbine power then directed towards hydrogen conversion. For Structure 3, a single test was conducted considering wind speed variations, as Structure 3 exclusively focuses on the offshore conversion of electrical energy into hydrogen.

The simulations aimed to ensure the proper operation and effectiveness of the proposed features in different operational scenarios.

5.1. Simulation Results for Structure 1

The simulation results for Structure 1 are shown in Figure 12. For the first case study, the wind speed was initially 11 m/s and increased to 13 m/s at t = 30 s. Figure 12 shows the power output of the wind turbine, the electrolyser power devoted to hydrogen production, and the electrical power consumption by the local load. As can be seen in Figure 12, 80% of the power produced by the offshore wind turbine is used for hydrogen production in the electrolyser and 20% is used to supply the grid, as proposed in the controller shown in Figure 10. As mentioned above, at t = 30 s the wind turbine power increases from 725 kW to 1200 kW, the power in the electrolyser increases from 580 kW to 960 kW, and the power supplied to the grid increases from 145 kW to 240 kW due to a change in wind speed from 11 m/s to 13 m/s.

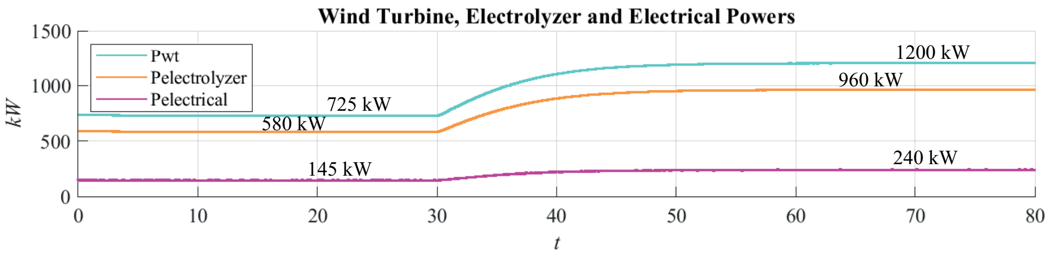

Figure 12. Power distribution for Structure 1 with priority on the electrolyser.

In the second case study, the same change in wind speed is considered at the same time as in the previous case. However, the focus now shifts to prioritising the electrical load. A reference power of 400 kW is established for electrical consumption, with any surplus power being channelled into hydrogen conversion. The power distributions for this case study are illustrated in Figure 13. This figure shows that both the wind turbine and electrolyser exhibit an increase in power from 725 kW to 1200 kW and from 325 kW to 800 kW, respectively, when the wind speed rises. The power assigned to the electrical load remains constant at 400 kW, notwithstanding the increase in the wind speed. Therefore, the controller maintains a steady electrical power supply to the electrical load while diverting any excess power towards hydrogen conversion.

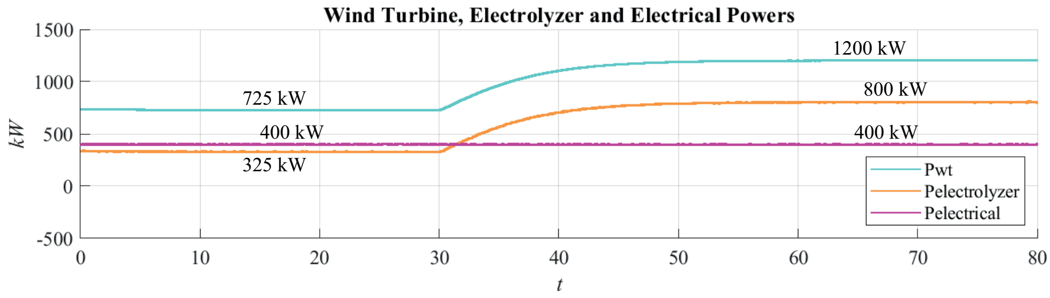

Figure 13. Power distribution for Structure 1 with priority on supplying electrical load.

5.2. Simulation Results for Structure 2

In Structure 2, hydrogen conversion takes place offshore and is subsequently transported onshore through a pipeline. The simulation results for this structure are shown in Figure 5 and the associated power distributions are illustrated in Figures 14 and 15. For the initial case study involving this structure, a change in wind speed was applied that ranged from 12 m/s to 14 m/s. As shown in Figure 14, similar to Structure 1, 80% of the wind turbine power (equivalent to 756 kW) is directed to the electrolyser, with the remaining 20% (amounting to 189 kW) supplied to the grid.

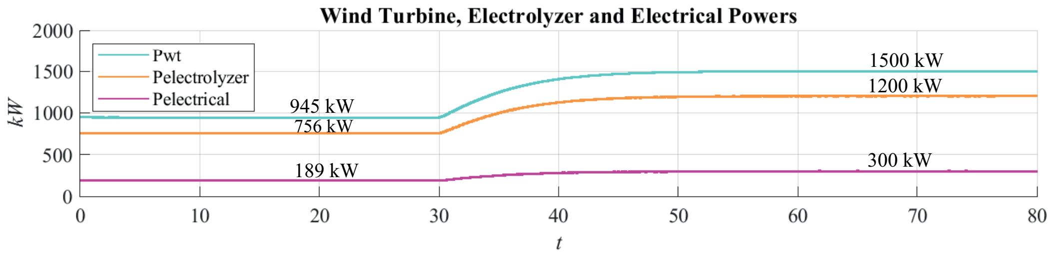

Figure 14. Power distribution for Structure 2 with priority on the electrolyser.

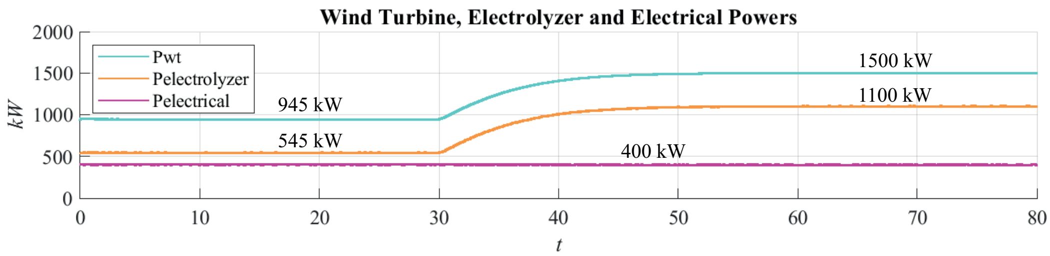

Figure 15. Power distribution for Structure 2 with priority on supplying electrical load.

The power levels for the second case study are shown in Figure 15. Similar to Structure 1, the aim of this case study was to ensure a specified power supply to the local loads, in this case 400 kW, with the surplus power being converted into hydrogen.

As depicted in Figure 15, the reference power for supplying the local power load was set at 400 kW and remained constant despite variations in the turbine power resulting from changes in the wind speed. In contrast, the power used by the electrolyser for hydrogen production increased from 545 kW to 1100 kW as the wind turbine power increased from 945 kW to 1500 kW.

5.3. Simulation Results for Structure 3

As shown in Figure 6, Structure 3 was simulated under the assumption that all power generated by the wind turbine is converted and transported into hydrogen. The results for this configuration are presented in Figure 16. As can be seen, the power generated by the wind turbine matches the power consumed by the electrolyser for hydrogen production. This configuration minimises the number of power conversion stages, and consequently the related cost and losses, though at the expense of losing the flexibility of electrical transmission.

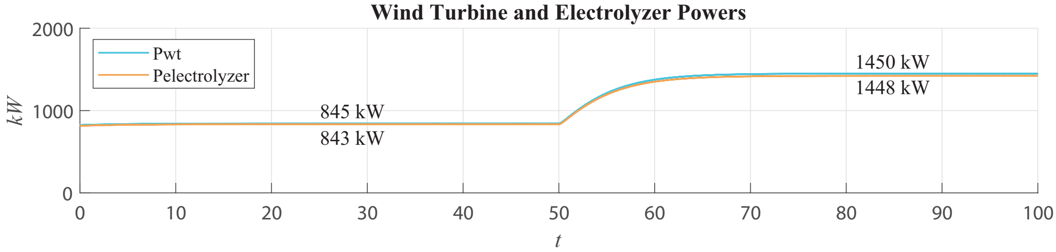

Figure 16. Power distribution for Structure 3 when dedicating the entire power output to the electrolyser.

An increase in wind speed from 10 m/s to 12 m/s occurs at t = 50 s, leading to an increase in the wind power production from 845 kW to 1450 kW. This power is solely utilised by the electrolyser, starting at 843 kW and increasing to 1448 kW following the wind speed increase.

5.4. Simulation Results for Structure 4

Structure 4 utilises DC power transmission for hydrogen production, with the corresponding simulation results presented in Figure 7. In the first case study, similar to the preceding structures, there is an increase in the wind speed, with 80% of the turbine power allocated for hydrogen production and the remaining 20% supplied to the grid. The power outputs corresponding to the wind turbine, electrolyser, and grid are illustrated in Figure 17.

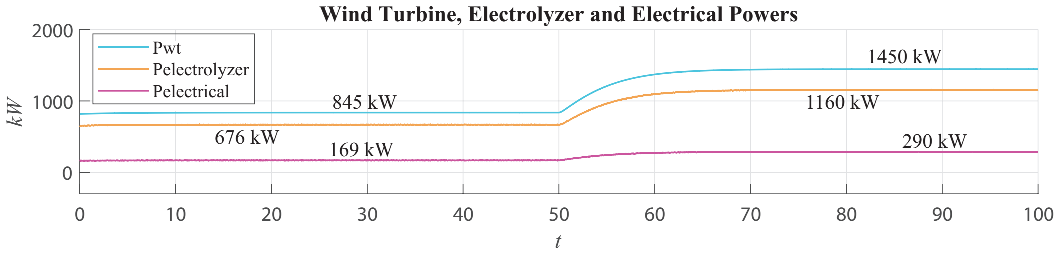

Figure 17. Power distribution for Structure 4 with priority on the electrolyser.

Prior to the change in wind speed, the wind turbine produces 845 kW, the electrolyser consumes 676 kW, and 169 kW is designated for supplying the grid. When the wind speed increases at t = 50, the power outputs change as follows: the wind turbine power production increases to 1450 kW, the electrolyser power consumption rises to 1160 kW, and the power for feeding the grid becomes 290 kW.

In the second case study for Structure 4, the approach prioritises supplying a 400 kW local load, with any remaining power directed to the electrolyser. As shown in Figure 18, the power supply to local loads is maintained at its reference value of 400 kW, with all surplus power used for green hydrogen production. Before the wind speed increase, the wind turbine power production is 845 kW and the electrolyser's power consumption is 445 kW. Following the wind speed step, the wind turbine power production increases to 1450 kW and the electrolyser's power consumption rises to 1050 kW.

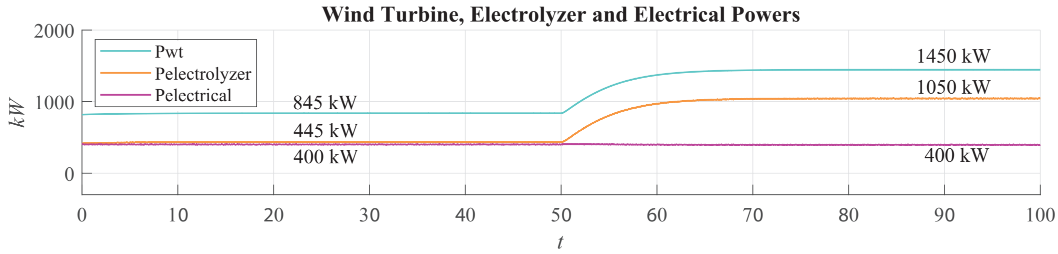

Figure 18. Power distribution for Structure 4 with priority on supplying electrical load.

6. Conclusions

Hydrogen is an energy carrier with great potential for the decarbonisation of the economy. There is significant potential for green hydrogen production from offshore wind farms, which have abundant renewable resources. When hydrogen is produced using wind power, it can be transported via pipelines alongside electricity through either AC or DC lines. This manuscript presents various architectures for energy transport taking into account the currently available technologies. Structure 1 utilises conventional AC lines with the electrolyser located onshore. In this configuration, a rectifier is required at the coast. Structure 2 employs AC lines with the electrolyser situated offshore, transporting the hydrogen to the coast via pipelines alongside electricity. Structure 3 bypasses electricity transmission entirely, directing all wind power towards hydrogen production, which is then transported to the coast through pipelines. Structure 4 considers DC lines with the electrolyser located onshore, minimising the number of power conversion stages.

The most significant outcome of this article is the development and evaluation of four different control structures for combined electricity and hydrogen production from offshore wind turbines. These structures regulate both electricity and hydrogen generation, utilising offshore wind power to its full potential.

The advantages of these structures are apparent in their customised approaches, with some designed for transmitting electricity and producing hydrogen onshore and others for optimising the entire conversion process offshore. For example, Structure 3 highlights energy transportation, as all the power generated by the wind turbine is converted into hydrogen, eliminating the need for electricity transmission. Transporting hydrogen over long distances using pipelines can incur fewer technical challenges compared to AC or DC transmission. Structure 4 also minimises energy losses by using direct current (DC) transmission, which reduces the need for AC–DC conversions and the associated energy losses.

Structures 1 and 2 use a more complex control mechanism that is applied to manage both AC and hydrogen transport. Our simulations show that these structures efficiently prioritise either hydrogen production or electricity distribution, ensuring reliable power management even as wind speeds change. In particular, Structure 1 demonstrates stable power distribution, with 80% of the generated power being used for hydrogen production, indicating that this structure is a reliable choice for consistent hydrogen production.

Structure 3 avoids the infrastructure and operational costs related to electricity transmission at the expense of moving the hydrogen production site offshore. This structure eliminates multiple conversion steps, as it focuses solely on offshore hydrogen production.

Unlike Structures 1 and 2, Structure 4 only considers DC transmission infrastructure and does not consider AC or hydrogen transport, which simplifies the power conversion process. Conversely, Structures 1 and 2 offer more flexibility by balancing hydrogen production with electricity generation.

Our simulation results highlight the performance differences between the four structures and support the case for using these control structures based on their specific operational applications. Each structure offers unique advantages depending on the specific offshore and onshore requirements, providing flexibility, interoperability, and enhanced integration of renewable energy sources.

Our comparative analysis of control strategies shows that Structures 1 and 2 have higher control complexity due to the need to manage both the rectifier and *dc–dc* converter.

This increases the number of components to be controlled, making overall system coordination more challenging. In contrast, Structure 4 reduces complexity by requiring fewer converters when considering PMSM. Structure 3 features the simplest control strategy, with only two controllers.

Our simulation results demonstrate the effective operation of the different structures following two strategies, namely, power sharing between electricity and hydrogen production and prioritising local load supply while delivering excess wind power to the grid. Future work could explore the use of grid-forming converters and high-power three-phase dual active bridges.

Author Contributions: All authors have made an important contribution to the creation of this paper. Conceptualization, J.L.M.-M. and R.P.-A.; methodology, J.L.M.-M., R.P.-A. and O.A.-L.; software, J.L.M.-M., R.P.-A. and D.C.-G.; validation, J.L.M.-M. and R.P.-A.; formal analysis, J.L.M.-M. and R.P.-A.; investigation, J.L.M.-M., R.P.-A., D.C.-G. and O.A.-L.; resources, J.L.M.-M. and R.P.-A.; data curation, J.L.M.-M. and R.P.-A.; writing—original draft preparation, J.L.M.-M., R.P.-A., D.C.-G. and O.A.-L.; writing—review and editing, J.L.M.-M., R.P.-A. and O.A.-L.; visualization, J.L.M.-M. and D.C.-G.; supervision, R.P.-A., D.C.-G. and O.A.-L.; project administration, R.P.-A., D.C.-G. and O.A.-L.; funding acquisition, J.L.M.-M. and R.P.-A. All authors have read and agreed to the published version of the manuscript.

Funding: This research received no external funding.

Data Availability Statement: The original contributions presented in the study are included in the article, further inquiries can be directed to the corresponding author/s.

Conflicts of Interest: The authors declare no conflicts of interest.

References

1. Ibrahim, O.S.; Singlitico, A.; Proskovics, R.; McDonagh, S.; Desmond, C.; Murphy, J.D. Dedicated large-scale floating offshore wind to hydrogen: Assessing design variables in proposed typologies. *Renew. Sustain. Energy Rev.* **2022**, *160*, 112310. [CrossRef]
2. Erdiwansyah; Mahidin; Husin, H.; Nasaruddin; Zaki, M.; Muhibbuddin. A critical review of the integration of renewable energy sources with various technologies. *Prot. Control Mod. Power Syst.* **2021**, *6*, 1–18.
3. Osman, A.I.; Chen, L.; Yang, M.; Msigwa, G.; Farghali, M.; Fawzy, S.; Rooney, D.W.; Yap, P.S. Cost, environmental impact, and resilience of renewable energy under a changing climate: A review. *Environ. Chem. Lett.* **2022**, *21*, 741–764. [CrossRef]
4. Calado, G.; Castro, R. Hydrogen production from offshore wind parks: Current situation and future perspectives. *Appl. Sci.* **2021**, *11*, 5561. [CrossRef]
5. Amaral, J.L. The Underwater Sound from Offshore Wind Farms. *Acoust. Today* **2020**, *16*, 13–21. [CrossRef]
6. Keivanpour, S.; Ramudhin, A.; Kadi, D.A. The sustainable worldwide offshore wind energy potential: A systematic review. *J. Renew. Sustain. Energy* **2017**, *9*, 065902. [CrossRef]
7. Díaz, H.; Soares, C. Review of the current status, technology and future trends of offshore wind farms. *Ocean Eng.* **2020**, *209*, 107381. [CrossRef]
8. Durakovic, G.; del Granado, P.C.; Tomasgard, A. Powering Europe with North Sea offshore wind: The impact of hydrogen investments on grid infrastructure and power prices. *Energy* **2023**, *263*, 125654. [CrossRef]
9. Cuevas, F.; Zhang, J.; Latroche, M. The vision of France, Germany, and the European Union on future hydrogen energy research and innovation. *Engineering* **2021**, *7*, 715–718. [CrossRef]
10. Fernández-González, R.; Puime-Guillén, F.; Panait, M. Multilevel governance, PV solar energy, and entrepreneurship: The generation of green hydrogen as a fuel of renewable origin. *Util. Policy* **2022**, *79*, 101438. [CrossRef]
11. Bhattacharyya, R.; Misra, A.; Sandeep, K. Photovoltaic solar energy conversion for hydrogen production by alkaline water electrolysis: Conceptual design and analysis. *Energy Convers. Manag.* **2017**, *133*, 1–13. [CrossRef]
12. Franco, A.; Giovannini, C. Recent and Future Advances in Water Electrolysis for Green Hydrogen Generation: Critical Analysis and Perspectives. *Sustainability* **2023**, 15, 16917. [CrossRef]
13. Hassan, N.; Jalil, A.A.; Rajendran, S.; Khusnun, N.F.; Bahari, M.B.; Johari, A.; Kamaruddin, M.; Ismail, M. Recent review and evaluation of green hydrogen production via water electrolysis for a sustainable and clean energy society. *Int. J. Hydrogen Energy* **2024**, *52*, 420–441. [CrossRef]
14. Kumar, S.S.; Lim, H. An overview of water electrolysis technologies for green hydrogen production. *Energy Rep.* **2022**, *8*, 13793–13813. [CrossRef]
15. Moosa, I.S.; Kazem, H.A.; Al-Iessi, L.M.R. Production of Hydrogen via Renewable Energy and Investigation of Water Molecular Changes During Electrolysis Process. *J. Renew. Energy Environ.* **2021**, *8*, 19–28.

16. Panchenko, V.; Daus, Y.V.; Kovalev, A.; Yudaev, I.; Litti, Y.V. Prospects for the production of green hydrogen: Review of countries with high potential. *Int. J. Hydrogen Energy* **2022**,*48*, 4551–4571. [CrossRef]
17. Arsad, A.Z.; Hannan, M.; Al-Shetwi, A.Q.; Mansur, M.; Muttaqi, K.; Dong, Z.; Blaabjerg, F. Hydrogen energy storage integrated hybrid renewable energy systems: A review analysis for future research directions. *Int. J. Hydrogen Energy* **2022**, *47*, 17285–17312. [CrossRef]
18. Ottersten, R. *On Control of Back-to-Back Converters and Sensorless Induction Machine Drives*; Chalmers University of Technology: Göteborg, Sweden, 2003.
19. Boldea, I. *Variable Speed Generator*; CRC Press: Boca Raton, FL, USA, 2009.
20. Yazdani, A.; Iravani, R. *Voltage-Sourced Converters in Power Systems: Modeling, Control, and Applications*; John Wiley & Sons: Hoboken, NJ, USA, 2010.
21. Anaya-Lara, O.; Campos-Gaona, D.; Moreno-Goytia, E.; Adam, G. *Offshore Wind Energy Generation: Control, Protection, and Integration to Electrical Systems*; John Wiley & Sons: Hoboken, NJ, USA, 2014.
22. ABDI YONIS, S.; Yusupov, Z.; Habbal, A.; Toirov, O. Control approach of a grid connected DFIG based wind turbine using MPPT and PI controller. *Adv. Electr. Electron. Eng.* **2023**, *21*, 157–170. [CrossRef]
23. binti Jefri, F.I.; Fujita, G. PI control system for input current of active rectifier in SST. In Proceedings of the 2017 5th International Conference on Electrical, Electronics and Information Engineering (ICEEIE), Malang, Indonesia, 6–8 October 2017; pp. 102–107.
24. Davari, P.; Zare, F.; Abdelhakim, A. Active rectifiers and their control. In *Control of Power Electronic Converters and Systems*; Elsevier: Amsterdam, The Netherlands, 2018; pp. 3–52.
25. Denis, K.; Olha, K.; Serhii, R. Active rectifier with different control system types. In Proceedings of the 2020 IEEE 4th International Conference on Intelligent Energy and Power Systems (IEPS), Istanbul, Turkey, 7–11 September 2020; pp. 273–278.
26. Rashid, M.H. *Electrónica de Potencia: Circuitos, Dispositivos y Aplicaciones*; University of Florida: Gainesville, FL, USA; Pearson Educación: London, UK, 2004.
27. Mohan, N.; Undeland, T.M.; Robbins, W.P. *Power Electronics: Converters, Applications, and Design*; John Wiley & Sons: Hoboken, NJ, USA, 2003.
28. Monroy-Morales, J.L.; Hernández-Ángeles, M.; Campos-Gaona, D.; Peña-Alzola, R.; Ordonez, M.; Mérida, W. Modeling and control design of a Vienna rectifier based electrolyzer. In Proceedings of the 2016 IEEE 7th International Symposium on Power Electronics for Distributed Generation Systems (PEDG), Vancouver, BC, Canada, 27–30 June 2016; pp. 1–8.
29. Jiang, W.; Wu, Y.K.; Yang, T.; Yu, F.; Wang, W.; Hashimoto, S. Identification and Power Electronic Module Design of a Solar Powered Hydrogen Electrolyzer. In Proceedings of the 2012 Asia-Pacific Power and Energy Engineering Conference, Shanghai, China, 27–29 March 2012; pp. 1–4.
30. Eraydin, H.; Bakan, A.F. Efficiency Comparison of Asynchronous and Synchronous Buck Converter. In Proceedings of the 2020 6th International Conference on Electric Power and Energy Conversion Systems (EPECS), Istanbul, Turkey, 5–7 October 2020; pp. 30–33.
31. Zomorodi, H.; Nazari, E. Design and Simulation of Synchronous Buck Converter in Comparison with Regular Buck Converter. *Int. J. Robot. Control. Syst.* **2022**, *2*, 79–86. [CrossRef]
32. Anuchin, A.; Shpak, D.; Ahmed, M.R.; Stolyarov, E.; Surnin, D.; Acedo, J.P. Nested Loop Control of a Buck Converter under Variable Input Voltage and Load Conditions. In Proceedings of the 2020 55th International Universities Power Engineering Conference (UPEC), Turin, Italy, 1–4 September 2020; pp. 1–5.
33. Rigogiannis, N.; Baros, D.; Lempesis, E.; Ntoga, S.; Peioglou, E.; Pechlivanis, C.; Papanikolaou, N.P. Experimental Investigation of a Digitally Current Controlled Synchronous Buck DC/DC Converter for Microgrids Applications. In Proceedings of the 2019 Panhellenic Conference on Electronics & Telecommunications (PACET), Volos, Greece, 8–9 November 2019; pp. 1–5.
34. Ulleberg, Ø. Modeling of advanced alkaline electrolyzers: A system simulation approach. *Int. J. Hydrogen Energy* **2003**, *28*, 21–33. [CrossRef]